5892 *Chem. Mater.* **2009,** *21,* 5892–5898
DOI:10.1021/cm903108h

CHEMISTRY OF MATERIALS
Article

Supramolecular Nanotube Hydrogels: Remarkable Resistance Effect of Confined Proteins to Denaturants

Naohiro Kameta,*[,†,‡] Kaname Yoshida,[§] Mitsutoshi Masuda,[†,‡] and Toshimi Shimizu*[,†,‡]

[†]*Nanotube Research Center (NTRC), National Institute of Advanced Industrial Science and Technology (AIST), Tsukuba Central 5, 1-1-1 Higashi, Tsukuba, Ibaraki 305-8565, Japan,* [‡]*SORST, Japan Science and Technology Agency (JST), Tsukuba Central 5, 1-1-1 Higashi, Tsukuba, Ibaraki 305-8565, Japan, and* [§]*Institute for Chemical Research (ICR), Kyoto University, Uji, Kyoto 611-0011, Japan*

Received October 8, 2009

Nanotube networks self-assembling from asymmetric bolaamphiphile, *N*-(β-D-glucopyranosyl)-*N*′-(2-glycylglycylglycineamideethyl)-octadecanediamide **1**, acted as hydrogelators. The obtained nanotube hydrogel was able to separately fix a green fluorescent protein (GFP) and a myoglobin (Mb) into not only independent nanospaces consisting of three-dimensional meshworks formed in between nanotubes but also a one-dimensional hollow cylinder of the nanotube itself. Especially, the fixed GFP and Mb into the nanotube hollow cylinder with 9 nm inner diameter showed strong resistance to denaturants such as guanidinium chloride and urea at high concentrations. The oxygen binding ability of the fixed Mb into the nanotube hollow cylinder was remarkably superior to those of the fixed Mb into the nanotube meshworks and the free Mb in bulk. The nanotube hydrogel also showed slow release behavior depending on pH conditions. Such a unique fixation property of the nanotube hydrogel has never been seen for preceded supramolecular and polymer hydrogels having three-dimensional meshworks formed in between nanofibers. Hence, the nanotube hydrogel can function as a novel soft material applicable to biological and medical fields.

Introduction

Supramolecular hydrogels, in which nanofiber networks self-assembling from low-molecular weight compounds act as gelators, should be more useful than polymer hydrogels in terms of their characteristics including facile preparation conditions without requiring polymerization, effective introduction of functions, and reversible sol−gel transformation by various external stimuli.[1,2] Especially, such smart hydrogels have attracted much attention in the field of biological and medical care, since the three-dimensional meshworks in the hydrogels function as a semiwet media for bioanalysis,[3] cell culture,[4] and a reservoir for drug-delivery system.[5] On the other hand, self-assembly of rationally designed synthetic amphiphiles in water can give tubular structures, which can well disperse in the aqueous solution.[6] The self-assembled nanotubes provide a well-defined one-dimensional hollow cylinder with 10−100 nm inner diameters[7] that is applicable as not only templates to fabricate metal nanowires and inorganic nanotubes[8] but also containers to preserve and release biomolecules,[9] or channels for pipets.[10] The character of the nanospace based on the nanotube hollow cylinder is remarkably different from that of the meshworks formed in between nanofibers of the supramolecular hydrogels as mentioned above, with respect to dimensionality. Hierarchical aggregation and entanglement of the nanotubes in water allow us to develop novel hydrogel implementing the attractive

*To whom correspondence should be addressed. Fax: +81-29-861-4545. E-mail: n-kameta@aist.go.jp (N.K.); tshmz-shimizu@aist.go.jp (T.S.).

(1) Weiss, R. G.; Terech, P. *MOLECULAR GELS, materials with self-assembled fibrillar networks*; Springer: Netherlands, 2006.
(2) Review: (a) Estroff, L. A.; Hamilton, A. D. *Chem. Rev.* **2006**, *104*, 1201–1217. (b) Sangeetha, N. M.; Maitra, U. *Chem. Soc. Rev.* **2005**, *34*, 821–836. (c) Hirst, A. R.; Smith, D. K. *Chem.—Eur. J.* **2005**, *11*, 5496–5508. (d) Loos, M. De.; Feringa, B. L.; Esch, J. H. van *Eur. J. Org. Chem.* **2005**, *17*, 3615–3631. (e) Zhao, F.; Ma, M. L.; Xu, B. *Chem. Soc. Rev.* **2009**, *38*, 883–891. (f) Suzuki, M.; Hanabusa, K. *Chem. Soc. Rev.* **2009**, *38*, 967–975.
(3) (a) Kiyonaka, S.; Sada, K.; Yoshimura, I.; Shinkai, S.; Kato, N.; Hamachi, I. *Nat. Mater.* **2004**, *3*, 58–64. (b) Ulijn, R. V. *J. Mater. Chem.* **2006**, *16*, 2217–2225. (c) Seo, Y. J.; Bhuniya, S.; Yi, J. W.; Kim, B. H. *Tetrahedron Lett.* **2008**, *49*, 2701–2703.
(4) (a) Silva, G. A.; Czeisler, C.; Niece, K. L.; Beniash, E.; Harrington, D. A.; Kessler, J. A.; Stupp, S. I. *Science* **2004**, *303*, 1352–1355. (b) Jayawarna, V.; Ali, M.; Jowitt, T. A.; Miller, A. F.; Saiani, A.; Gough, J. E.; Ulijn, R. V. *Adv. Mater.* **2006**, *18*, 611–614. (c) Mahler, A.; Reches, M.; Rechter, M.; Cohen, S.; Gazit, E. *Adv. Mater.* **2006**, *18*, 1365–1370. (d) Ikeda, M.; Ueno, S.; Matsumoto, S.; Shimizu, Y.; Komatsu, H.; Kusumoto, K.-i.; Hamachi, I. *Chem.—Eur. J.* **2008**, *14*, 10808–10815.
(5) (a) Haines-Butterick, L.; Rajagopal, K.; Branco, M.; Salick, D.; Rughani, R.; Pilarz, M.; Lamm, M. S.; Pochan, D. J.; Schneider, J. P. *Proc. Natl. Acad. Sci. U.S.A.* **2007**, *104*, 7791–7796. (b) Li, X.; Li, J. *J. Biomed. Mater. Res.* **2007**, *86A*, 1055–1061. (c) Shankar, B. V.; Patnaik, A. *J. Phys. Chem. B* **2007**, *111*, 9294–9300. (d) Vemula, P. K.; Cruikshank, G. A.; Karp, J. M.; John, G. *Biomaterials* **2009**, *30*, 383–393.
(6) Review: Shimizu, T.; Masuda, M.; Minamikawa, H. *Chem. Rev.* **2005**, *105*, 1401–1443.
(7) Review: (a) Shimizu, T. *J. Polym. Sci. Part A* **2006**, *44*, 5137–5152. (b) Shimizu, T. *J. Polym. Sci. Part A* **2008**, *46*, 2601–2611.
(8) Review: (a) Guo, X.; Matsui, H. *Adv. Mater.* **2005**, *17*, 2037–2050. (b) Zhou, Y.; Shimizu, T. *Chem. Mater.* **2008**, *20*, 625–633.
(9) (a) Hurtig, J.; Orwar, O. *Soft Matter* **2008**, *4*, 1515–1520. (b) Kameta, N.; Minamikawa, H.; Masuda, M.; Mizuno, G.; Shimizu, T. *Soft Matter* **2008**, *4*, 1681–1687.
(10) Nogawa, K.; Tagawa, Y.; Nakajima, M.; Arai, F.; Shimizu, T.; Kamiya, S.; Fukuda, T. *J. Robot. Mechatronics* **2007**, *19*, 528–534.

Published on Web 11/04/2009

Scheme 1

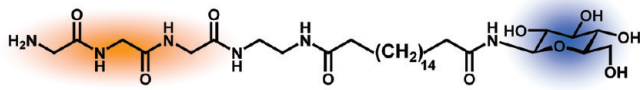

functions of the hollow cylinder. Such a hydrogel, "supramolecular nanotube hydrogel", has never been reported until now, although some nanotubes are known to be able to gelate organic solvents or mixture of water and polar organic solvents.[11]

Here, we have demonstrated for the first time the self-assembly of supramolecular nanotube hydrogels consisting of a novel asymmetric bolaamphiphile **1** (Scheme 1) by pH control under room temperature conditions. We discuss the unique fixation property of proteins by the supramolecular nanotube hydrogels which have independent nanospaces, i.e., the three-dimensional meshworks formed in between nanotubes and the one-dimensional hollow cylinder of the nanotube itself.

Results and Discussion

Formation of the Nanotube Hydrogel. We already found that symmetric bolaamphiphiles, having two identical hydrophilic headgroups such as sugar, peptide, or oligonucleotide at both ends of a long alkyl spacer, self-assemble into nanofibers acting as good hydrogelators.[12] Here we have newly designed and synthesized an asymmetric bolaamphiphile **1** composed of glucose and triglycine headgroups, since the asymmetry based on both headgroups of different size can induce the nanotube formation with spray-typed molecular packing.[13] The self-assembly of **1** in water was carried out by only changing the pH conditions at room temperatures. The hydrochloride salt of **1** was dissolved in water (5 mg/mL) at pH 5. Addition of NaOH to adjust the aqueous solution to pH 8 instantly transformed the resultant clear solution of **1** to a hydrogel (Figure 1a). Cryo-transmission electron microscopic (cryo-TEM) observation for the obtained hydrogel revealed the formation of fiber structures of ca. 15 nm in width (Figure 1b). Scanning electron microscopic (SEM) observation for the xerogel displays well-defined open ends in the fibers (Figures 1c and d), indicating that the self-assembled morphologies in the hydrogel are identified as a tubular structure. The penetration of the negative staining reagent, phosphotungstate, into the hollow cylinder can strongly support the tubular structure with two open ends (Figure 1e). Thus, the tubular structures are easily distinguishable from the fiber structures by using TEM observation. The tubular structures have 9-nm inner diameters and 3-nm membrane thickness and are several tens of micrometers in length. The outer diameter (ca. 15 nm) estimated from the TEM image corresponds to the width of the fibers observed in the cryo-TEM image. IR measurements were performed to clarify the molecular packing of the nanotubes. The spectrum indicates two peaks at 1420 and 1026 cm^{-1} assignable to the CH deformation and skeletal vibration bands[14] of the triglycine moieties of **1**, suggesting that **1** forms polyglycine-II-type hydrogen bonding[15] (Supporting Information). This specific intermolecular hydrogen bonding ensures parallel molecular packing in the nanotube.[16] The $\delta(CH_2)$ scissoring and $\gamma(CH_2)$ rocking vibration bands give a single sharp peak at 1465 and 719 cm^{-1}, respectively, suggesting that the lateral chain packing of the oligomethylene spacer in **1** is of a triclinic parallel type.[17] The subcell structure strongly supports the parallel molecular packing.[13c] The membrane thickness (3 nm) is thinner than that estimated from an extended molecular length (4.64 nm) of **1**. Therefore **1** tilts about 40° and packs in a parallel fashion within a single monolayer of the nanotubes. All results suggest that the nanotubes consist of a molecular monolayer membrane and have different inner and outer surfaces covered with triglycine and glucose headgroups, respectively (Figure 1f). Self-assembly of preceded nanotubes generally need a heating procedure to temperatures above phase transition of the amphiphiles. On the other hand, the sol−gel transition of the present supramolecular nanotube hydrogel is controllable by pH conditions at room temperatures, i.e., the protonation and deprotonation of the amino groups in the triglycine moieties.

Fixation of Green Fluorescent Protein into the Supramolecular Nanotube Hydrogel. Such an on-demand self-assembly process of the supramolecular nanotube hydrogel should be suitable for fixation and encapsulation of biomacromolecules. First, we investigated potential activity of the supramolecular nanotube hydrogel as an encapsulating soft material for fixation of proteins in terms of the resistance against denaturants. We chose a green fluorescent protein (GFP; *Aequorea victoria*, *recombinant*,

(11) (a) Wade, R. H.; Terech, P.; Hewat, E. A.; Ramasseul, R.; Volino, F. *J. Colloid Interface Sci.* **1985**, *107*, 244–255. (b) Jung, J. H.; Ono, Y.; Shinkai, S. *J. Chem. Soc. Perkin Trans. 2* **1999**, 1289–1291. (c) Bao, C.; Lu, R.; Jin, M.; Xue, P.; Tan, C.; Zhao, Y.; Liu, G. *Carbohydr. Res.* **2001**, *339*, 1311–1316. (d) Boettcher, C.; Schade, B.; Fuhrhop, J.-H. *Langmuir* **2001**, *17*, 873–877. (e) Jin, W.; Fukushima, T.; Niki, M.; Kosaka, A.; Ishii, N.; Aida, T. *Proc. Natl. Acad. Sci. U.S.A.* **2005**, *102*, 10801–10806. (f) Tzokova, N.; Fernyhough, C. M.; Topham, P. D.; Sandon, N.; Adams, D. J.; Butler, M. F.; Armes, S. P.; Ryan, A. J. *Langmuir* **2009**, *25*, 2479–2485.

(12) (a) Kogiso, M.; Hanada, T.; Yase, K.; Shimizu, T. *Chem. Commun.* **1998**, 1791–1792. (b) Jung, J. H.; Shinkai, S.; Shimizu, T. *Chem.—Eur. J.* **2002**, *8*, 2684–2690. (c) Iwaura, R.; Yoshida, K.; Masuda, M.; Yase, K.; Shimizu, T. *Chem. Mater.* **2002**, *14*, 3047–3053. (d) Iwaura, R.; Yoshida, K.; Masuda, M.; Ohnishi-Kameyama, M.; Yoshida, M.; Shimizu, T. *Angew. Chem., Int. Ed.* **2003**, *42*, 1009–1012.

(13) (a) Masuda, M.; Shimizu, T. *Langmuir* **2004**, *20*, 5969–5977. (b) Kameta, N.; Masuda, M.; Minamikawa, H.; Goutev, N. V.; Rim, J. A.; Jung, J. H.; Shimizu, T. *Adv. Mater.* **2005**, *17*, 2732–2736. (c) Kameta, N.; Masuda, M.; Minamikawa, H.; Shimizu, T. *Langmuir* **2007**, *23*, 4634–4641.

(14) (a) Blout, E. R.; Linsley, S. G. *J. Am. Chem. Soc.* **1952**, *74*, 1946–1951. (b) Bamford, C. H.; Brown, L.; Cant, E. M.; Elliott, A.; Hanby, W. E.; Malcolm, B. R. *Nature* **1955**, *176*, 396–397. (c) Crick, F. H. C.; Rich, A. *Nature* **1955**, *176*, 780–781.

(15) (a) Navarro, E.; Tereshko, V.; Subirana, J. A.; Puiggali, J. *Biopolymers* **1955**, *36*, 711–722. (b) Kogiso, M.; Ohnishi, S.; Yase, K.; Masuda, M.; Shimizu, T. *Langmuir* **1998**, *14*, 4978–4986. (c) Kogiso, M.; Masuda, M.; Shimizu, T. *Supramol. Chem.* **1998**, *9*, 183–189.

(16) Kameta, N.; Mizuno, G.; Masuda, M.; Minamikawa, H.; Kogiso, M.; Shimizu, T. *Chem. Lett.* **2007**, *36*, 896–897.

(17) (a) Garti, N.; Sato, K. *Crystallization and Polymorphism of Fats and Fatty Acids*; Mercel Dekker: New York, 1988; p 139. (b) Yamada, N.; Okuyama, K.; Serizawa, T.; Kawasaki, M.; Ohshima, S. *J. Chem. Soc. Perkin Trans. 2* **1996**, *12*, 2707–2713.

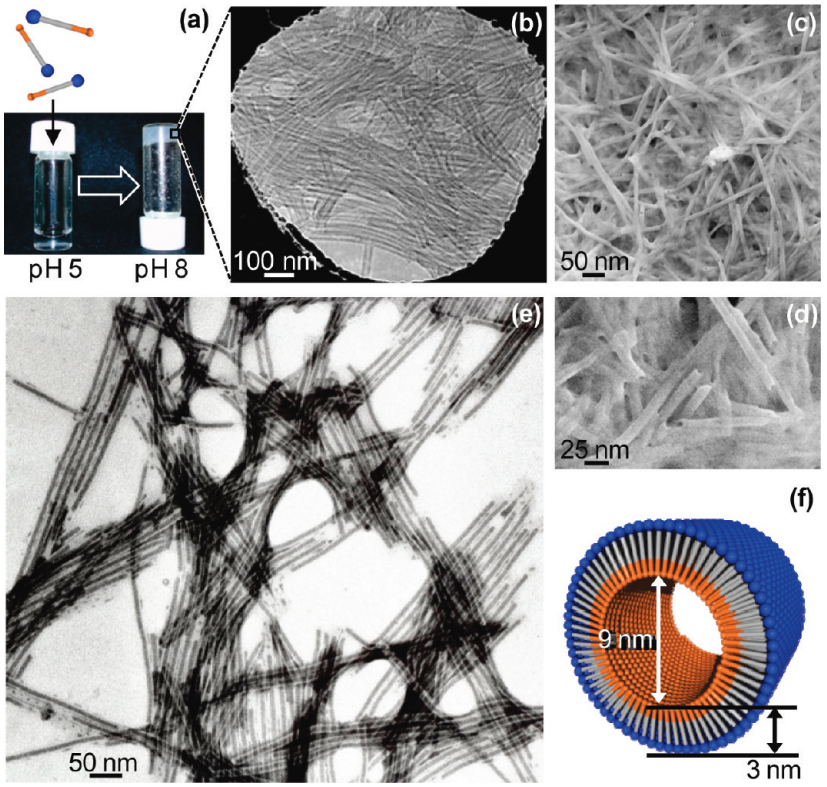

Figure 1. (a) Photograph of the pH-dependent nanotube hydrogel. (b) Cryo-TEM image of the nanotube hydrogel. (c and d) SEM image of the nanotube xerogel. (e) TEM image of the nanotubes dispersed from the hydrogel. (f) Model of the molecular monolayer nanotube.

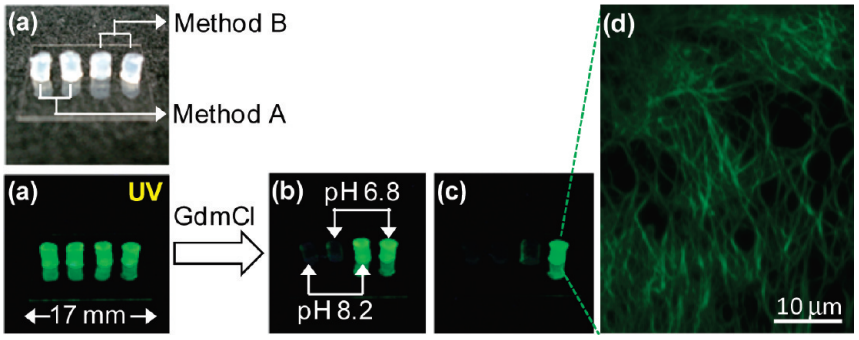

Figure 2. (a) Lumps of the nanotube hydrogels fixing GFP. (b and c) Lumps of the nanotube hydrogels fixing GFP upon addition of GdmCl. [GdmCl] = 6 mol L^{-1}. The standing time after addition of GdmCl is 1 h and 7 days, respectively. (d) Fluorescence microscopic image of the nanotube hydrogels fixing GFP after 7 days upon addition of GdmCl.

Upstate) as a target protein, since the biological and physicochemical properties are well-known.[18] Native GFP strongly fluoresces at 510 nm, whereas it sharply becomes nonfluorescence upon denaturation. We performed the fixation of GFP using the following two different methodologies. Method A follows the addition of GFP into the preformed supramolecular nanotube hydrogel. In method B, GFP is added in advance into the aqueous solution of **1** at pH 5, and then the resultant mixing solution was transformed to the supramolecular nanotube hydrogel by pH adjustment as described above. Four lumps of hydrogels (2 mm i.d. × 3 mm height) containing GFP prepared by methods A and B were placed on a glass plate (Figure 2a). Guanidinium chloride (total concentration of GdmCl: 6 mol L^{-1}) as a cationic denaturant was infused into each hydrogel lump using a syringe. Then, the pH was adjusted to 6.8 for two of four lumps and 8.2 for the remaining two lumps. The hydrogel prepared by method A (abbreviated as hydrogel A hereafter) immediately lost the fluorescence of GFP independent of the pH condition (Figures 2b and 3), indicating that GFP was almost denatured by GdmCl. On the other hand, the hydrogel prepared by method B (abbreviated as hydrogel B hereafter) kept the fluorescence of GFP for 1 h after standing. The quenching ratio of the fluorescence intensity was about 30% (Figure 3). The difference in the denaturation behavior between hydrogels A and B significantly depends on the restricted environment of GFP in the supramolecular nanotube hydrogel. Since the

(18) Chalfie, M.; Kain, S. R. *Green Fluorescent Protein: Properties, Applications, and Protocols*; Wiley-Interscience: New Jersey, 2006.

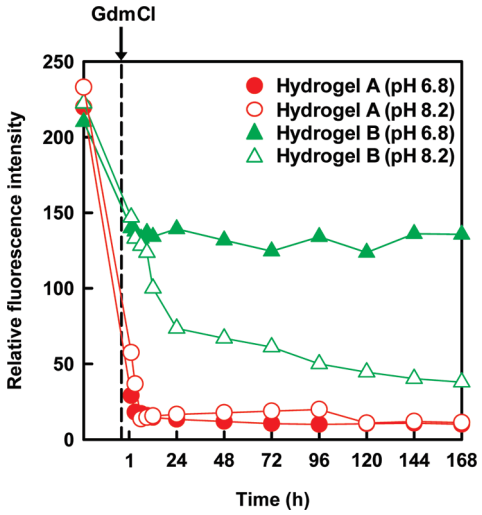

Figure 3. Time dependence of the relative fluorescence intensity (510 nm) of the fixed GFP in the nanotube hydrogels upon addition of GdmCl. The dotted line indicates the time when GdmCl is infused. Excitation wavelength: 398 nm.

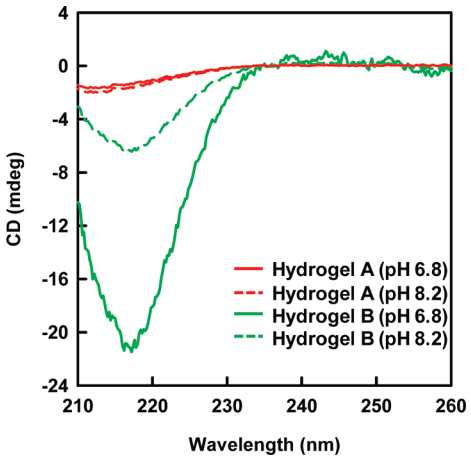

Figure 4. CD spectra of the fixed GFP in the nanotube hydrogels after 7 days upon addition of GdmCl.

denaturation of GFP in hydrogel A occurred smoothly, the GFP should be fixed into the three-dimensional meshworks formed in between nanotubes, where GdmCl was able to access it easily (Figure 5). In the case of hydrogel B, the formation of the nanotube hydrogel in the presence of GFP enabled us to encapsulate GFP by 70% in weight into the one-dimensional hollow cylinder of the nanotube itself (Figure 5). As a result, the fixed GFP in the nanotube hollow cylinder strongly refrained from contact with the GdmCl. The fast denaturation of the hydrogel B mentioned above corresponds to the fixed GFP (30%) into the three-dimensional meshworks formed in between nanotubes, which was similarly observed in hydrogel A. However, the pH conditions remarkably influenced the denaturation behavior after standing for a long time. The fluorescence of hydrogel B at pH 8.2 gradually decreased with the lapse of time, whereas the fluorescence at pH 6.8 remained even after 7 days (Figures 2c and 3). Fluorescence microscopic observation clearly showed strong fluorescence derived from native GFP along the high-axial direction of the nanotubes (Figure 2d), in which the tubular morphology without decomposition was confirmed by TEM observation (Supporting Information). Circular dichroism (CD) spectroscopy is also useful to monitor the denaturation behavior of proteins. The native GFP in a folding state has a strong CD band at around 215 nm based on a highly ordered conformation, whereas the denatured GFP in a defolding state gives very weak one. Actually, the CD spectra indicate that hydrogel B at pH 6.8 retains the strong CD activity after 7 days, while hydrogel B at pH 8.2, as well as hydrogel A, considerably loses the CD signal (Figure 4). At pH 6.8, the positively charged inner surface of the nanotubes by the protonation of the amino groups can effectively preserve negatively charged GFP via electrostatic attraction.[9b] The positive charge of the nanotube should also prevent penetration of cationic GdmCl into the hollow cylinder encapsulating GFP via electrostatic repulsion. At pH 8.2, the disappearance of the above electrostatic attraction and repulsion due to the deprotonation of the amino groups will induce not only the slow release[9b] of the GFP from the hollow cylinder to the outside but also the penetration of GdmCl into the hollow cylinder via a concentration gradient as the driving force. To elucidate the release of GFP and the penetration of GdmCl against the slow denature phenomena as observed at pH 8.2, we also performed the same experiment by using urea instead of cationic GdmCl as a neutral denaturant. Infusion of the urea (6 mol L^{-1}) into the hydrogel A caused the disappearance of the GFP fluorescence at pH 6.8 and 8.2 (Supporting Information). This means that the denaturation ability of urea toward the fixed GFP into the nanotube meshworks in the hydrogel is similar to that of GdmCl. The fixed GFP in the hydrogel B in the presence of urea showed nondenaturation at pH 6.8 and a slow denaturation at pH 8.2, respectively (Supporting Information). The nondenaturation shows a striking phenomenon, since nonionic urea could reach to the location of the encapsulating GFP via concentration gradient. This result at pH 6.8 strongly supports the idea that the GFP encapsulated into the nanotube hollow cylinder highly resists denaturation in the presence of the urea, whereas the fixed one in the nanotube meshworks never stabilizes.

We already demonstrated that confined water in a nanotube hollow cylinder, which has inner and outer surfaces covered with identical glucose headgroups, possesses a relatively higher viscosity and lower polarity as compared with bulk water.[19] Such characteristics of the confined water should stabilize the hydration structure of the GFP even though urea and GdmCl are well-known to denature GFP through effective destruction of the hydration structure. Furthermore, we found that the GFP and spherical protein encapsulated in the nanotube hollow cylinder, which has cationic inner surface covered with amino headgroup, diffuses slowly[20] and shows high

(19) Yui, H.; Guo, Y.; Koyama, K.; Sawada, T.; John, G.; Yang, B.; Masuda, M.; Shimizu, T. *Langmuir* **2005**, *21*, 721–727.
(20) Kameta, N.; Masuda, M.; Minamikawa, H.; Mishima, Y.; Yamashita, I.; Shimizu, T. *Chem. Mater.* **2007**, *19*, 3553–3560.

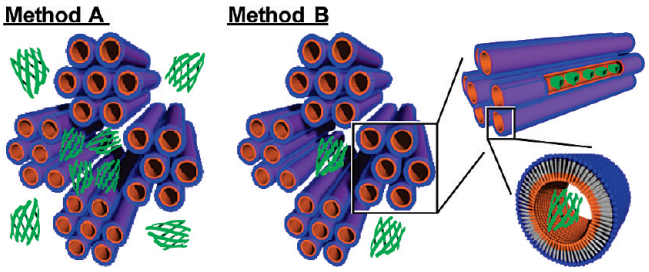

Figure 5. Schematic illustration of the fixed GFP in the three-dimensional meshworks and the one-dimensional hollow cylinder of the nanotube hydrogels.

thermal stability[21] based on the confinement effect. Restricted geometry of the nanotube hollow cylinder will also lead to kinetically and thermodynamically prevent the denaturation of the proteins. Similar denaturation resistance has been reported on various proteins encapsulated into mesoporous silica,[22] although to date the mechanism has never been cleared. Therefore, the slow denaturation observed in the hydrogel B at pH 8.2 is attributable to contact of the slowly released GFP from the nanotube hollow cylinder with urea or GdmCl existing outside (the meshworks) of the nanotubes.

Fixation of Mb into the Supramolecular Nanotube Hydrogel. Myoglobin (Mb, from equine heart), oxygen storage hemoprotein, was also chosen as a guest protein, since we can directly monitor its biological function by UV/vis spectroscopy.[23] We performed the fixation of Mb using the two same methods as described in for GFP. The supramolecular nanotube hydrogel transformed from the mixing solution of **1** and Mb by pH adjustment (abbreviated as hydrogel D hereafter) was purified with water through a decantation procedure to remove the fixed Mb into the nanotube meshworks (Supporting Information). Another method follows the addition of Mb into the preformed hydrogel (abbreviated as hydrogel C hereafter). The amount of the fixed Mb into the hydrogel C was controlled to be equal with that of the encapsulated Mb into the hydrogel D. Urea (1 mol L^{-1}) was infused into each hydrogel. Then, the pH and salt concentration were adjusted to 7.2 (50 mmol L^{-1} phosphate-buffered saline) and 150 mmol L^{-1} NaCl, respectively.

To evaluate the oxygen binding ability, we reduced a metmyoglobin (met-Mb) to a deoxymyoglobin (deoxy-Mb) using $Na_2S_2O_4$ (5 equiv.) Upon addition of $Na_2S_2O_4$ to each hydrogel, the Soret band of met-Mb at 409 nm shifted to that of deoxy-Mb at 434 nm (Figure 6), indicating that $S_2O_4^-$ acts as a reductant in both the nanotube meshworks and the nanotube hollow cylinder. Next, the introduction of O_2 for 5 min to the hydrogel D induced the blue-shift of the Soret band to 413 nm and the change in the shape of the Q-band around 550 nm

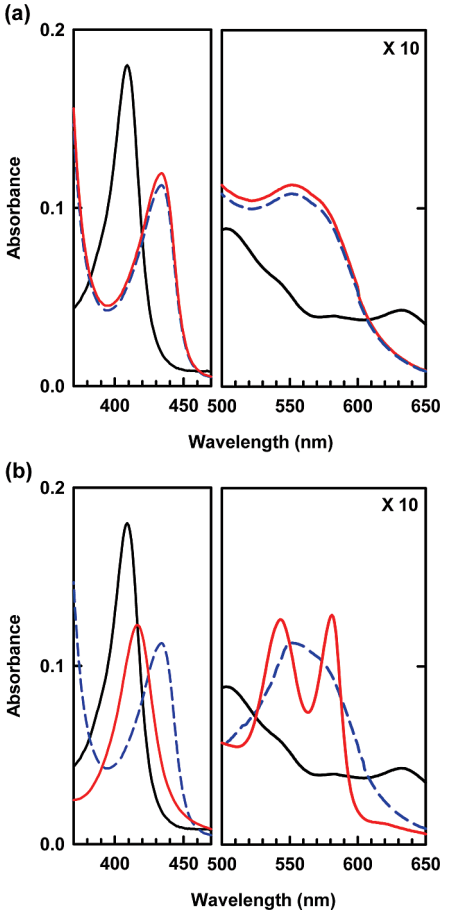

Figure 6. (a) Absorption spectra of the fixed Mb into the nanotube meshworks of the hydrogel C in the presence of urea: (black line) met-Mb; (blue line) after reduction of met-Mb via 5 equiv $S_2O_4^-$ (deoxy-Mb); (red line) O_2 introduction to deoxy-Mb. [fixed Mb] = 17 μg mL^{-1}, [urea] = 1 mol L^{-1}. (b) Absorption spectra of the encapsulated Mb into the nanotube hollow cylinder of the hydrogel D in the presence of urea: (black line) met-Mb; (blue line) after reduction of met-Mb via $S_2O_4^-$ (deoxy-Mb); (red line) O_2 introduction to deoxy-Mb (oxy-Mb). [fixed Mb] = 17 μg mL^{-1}, [urea] = 1 mol L^{-1}.

(Figure 6b). Such spectral change supported the encapsulated deoxy-Mb into the nanotube hollow cylinder binds O_2 and form oxymyoglobin (oxy-Mb) even though urea exists in the same location (Figure 7). On the other hand, the introduction of O_2 to the hydrogel C never brought similar spectral change (Figure 6a), showing that the fixed deoxy-Mb in the nanotube meshworks loses the oxygen binding ability because of the denaturation via urea (Figure 7).

The oxygenation/deoxygenation cycle of the fixed Mb into the hydrogel D was also monitored using the spectral change, which shows the appearance and disappearance of the absorption bands corresponding to oxy-Mb (red spectrum in Figure 6b) and deoxy-Mb (blue spectrum in Figure 6b). Figure 8 reveals that under harsh operating conditions of denaturation with urea, the encapsulated Mb in the nanotube hollow cylinder is able to repeatedly bind and release O_2 depending on the alternating introduction of O_2 gas for 30 min and Ar gas for 2 h, respectively.

In order to investigate the lifetime of the active Mb in various media, we traced the auto-oxidation reaction

(21) Kameta, N.; Masuda, M.; Mizuno, G.; Morii, N.; Shimizu, T. *Small* **2008**, *4*, 561–565.
(22) Review: Hudson, S.; Cooney, J.; Magner, E. *Angew. Chem., Int. Ed.* **2008**, *47*, 8582–8594.
(23) (a) Yamazaki, I.; Yokota, K.; Shikama, K. *J. Biol. Chem.* **1964**, *239*, 4151–4153. (b) Shikama, K.; Matsuoka, A. *J. Mol. Biol.* **1989**, *209*, 489–491.

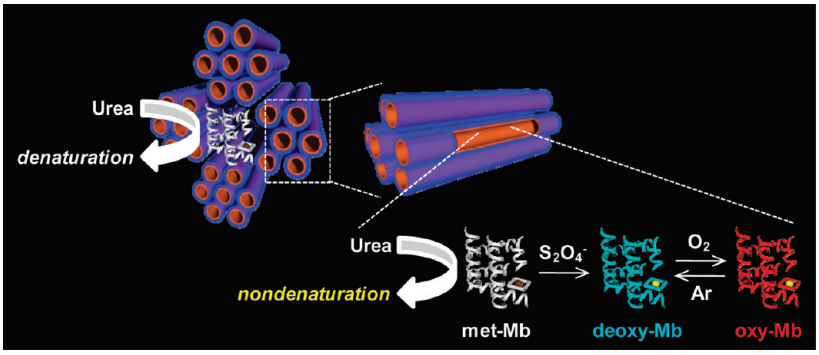

Figure 7. Schematic illustration of the fixed Mb into the three-dimensional meshworks and the one-dimensional hollow cylinder of the nanotube hydrogels.

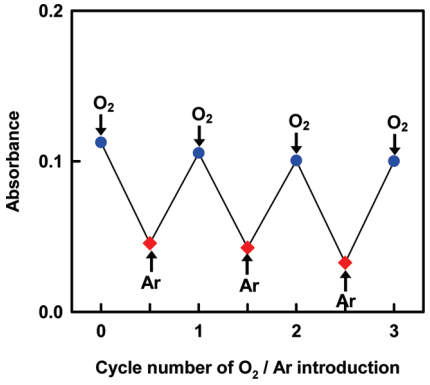

Figure 8. Change in the absorbance at 434 nm of the fixed Mb into the nanotube hollow cylinder of the hydrogel D in the presence of urea by the alternating introduction of O_2/Ar gas.

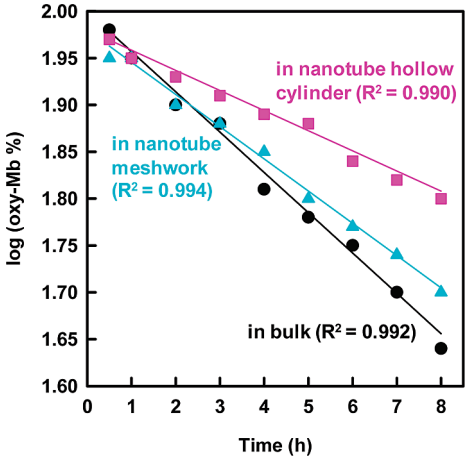

Figure 9. Time course of the auto oxidation of free oxy-Mb in bulk (black circle), the fixed oxy-Mb into the nanotube meshworks of the hydrogel C (blue triangle), and the fixed Mb into the nanotube hollow cylinder of the hydrogel D (pink square). Each line indicates a linear fitting curve.

from oxy-Mb to met-Mb in the supramolecular nanotube hydrogel by UV/vis spectroscopy. Absorbance of the two peaks (540 and 580 nm) in the Q-band for the fixed oxy-Mb into the hydrogel C, the hydrogel D, and free Mb in bulk in the absence of urea slowly decreased with increasing absorbance of two peaks (505 and 635 nm) assignable to met-Mb (Supporting Information). Since two isosbestic points were observed at 525 and 595 nm, the reaction obeys a typical single-exponential decay. Actually, the relationship between the time course and the logarithmic value of oxy-Mb percent gave linear lines (Figure 9). On the basis of the slope analysis, we calculated the rate constants (k_{ox}) to be 0.1, 0.08, and 0.05 for in bulk, in hydrogel C, and in hydrogel D, respectively. The half lifetime (τ = 8.8 h) of the fixed oxy-Mb into the nanotube meshworks of the hydrogel C is comparable to that (τ = 8.7 h) of the fixed oxy-Mb into the nanofiber meshworks of the precedent supramolecular nanofiber hydrogel.[24] In the case of the hydrogel D, the half lifetime (τ = 14 h) is obviously longer than that in the hydrogel C and that (free oxy-Mb, τ = 7.0 h) in bulk. The stable activity of the encapsulated oxy-Mb into the nanotube hollow cylinder will be attributable to the lowering of the nucleophilic attack of water molecules to the heme, since the water confined in the nanotube hollow cylinder possess the higher viscosity as described in the previous section.[19]

The supramolecular nanotube hydrogel was able to stabilize Mb while maintaining the long active state, whereas the activity of proteins has been often partially lost upon fixation by the conventional polymer hydrogels.[25]

Conclusion

We have for the first time succeeded in the construction of supramolecular nanotube hydrogel by self-assembly of the asymmetric bolaamphiphile **1**. The pH-dependent nanotube hydrogel was able to separately fix a protein into not only independent nanospaces consisting of three-dimensional meshworks formed between the nanotubes but also one-dimensional hollow cylinder of the nanotube itself. The unique property such as protein stabilization by encapsulation and slow release of a fixed protein without deformation of the nanotube hydrogel have never been seen for preceded supramolecular and polymer hydrogels having three-dimensional meshworks formed in between nanofibers. Therefore, the nanotube hydrogel as a novel soft material is widely applicable to biological and medical nanotechnologies.

(24) Kiyonaka, S.; Shinkai, S.; Hamachi, I. *Chem.—Eur. J.* **2003**, *9*, 976–983.

(25) (a) Tosa, T.; Sato, T.; Mori, T.; Yamamoto, K.; Takata, I.; Nishida, Y.; Chibata, I. *Biotechnol. Bioeng.* **1979**, *21*, 1697–1709. (b) Nishikawa, T.; Akiyoshi, K.; Sunamoto, J. *Macromolecules* **1994**, *27*, 7654–7659.

Experimental Section

Synthesis of *N*-(*β*-D-Glucopyranosyl)-*N′*-(2-glycylglycylglycine-amideethyl)-octadecane-diamide 1. The precursor, *N*-(2-aminoethyl)-*N′*-(2, 3, 4, 6-tetra-*O*-acetyl-*β*-D-glucopyranosyl)-octadecanediamide was synthesized as reported previously.[13c] The precursor was coupled with *Z*-GlyGlyGly-OSu (Bachem) in dimethylformamide at room temperature and purified by recrystallization. Removal of all protecting groups by methanolysis and hydrogenation gave **1**. ^{1}H NMR (400 MHz, DMSO-d_6, δ): 8.62 (t, 1H; NH), 8.27 (t, 1H; NH), 8.24 (d, 1H; NH), 7.91 (t, 1H; NH), 7.84 (t, 1H; NH), 4.96 (d, 1H; OH-4), 4.87 (d, 1H; OH-3), 4.81 (d, 1H; OH-2), 4.69 (t, 1H; H-1), 4.47 (t, 1H; OH-6), 3.85 (d, 2H; $NCH_2C{=}O$), 3.68 (d, 2H; $NCH_2C{=}O$), 3.63 (m, 1H; H-6), 3.60 (s, 2H; $NCH_2C{=}O$), 3.40 (m, 1H; H-6), 3.16 (m, 1H; H-4), 3.08 (m, 4H; NCH_2CH_2N), 3.0 (m, 3H; H-2, H-3, H-5), 2.04 (m, 4H; $CH_2C{=}O$), 1.47 (m, 4H; CH_2), 1.24 (m, 24H; CH_2). IR (cm^{-1}): 3291, 2918, 2849, 1641, 1549, 1465, 1447, 1420, 1382, 1283, 1250, 1082, 1026, 948, 894, 719, 691. ESI-MS (*m*/*z*): 689.7 $[M + H]^+$. Anal. calcd for $C_{32}H_{60}N_6O_{10}$: C 55.79, H 8.78, N 12.20. Found: C 55.68, H 8.85, N 12.07.

Cryo-TEM Observation. The nanotube hydrogel was dropped onto a microgrid and frozen by soaking in liquid nitrogen. The nanotubes embedded in the ice were observed by cryo-TEM (JEOL, JEM4000SFX) at 400 kV.

TEM Observation. The aqueous dispersion of the nanotube hydrogel was dropped onto a carbon grid and dried by standing at room temperature. The nanotubes, negatively stained with a phosphotungstate solution (2 wt %, pH adjusted to 9 by NaOH), were observed by TEM (Hitachi, H-7000) at 75 kV.

SEM Observation. The nanotube hydrogel was lyophilized, and then, the resultant xerogel was dropped onto the grid. The nanotubes were observed by SEM (Carl Zeiss, FE-SEM Supra 40) at 1 kV equipped with a chamber SE detector (SE2 mode).

Fluorescence Microscopic Observation. Fluorescence microscopic observation for the fixed GFP in the hydrogel in the presence of GdmCl by method B was performed using an inverted microscope (Olympus IX71) equipped with a CCD camera (Hamamatsu ORCA-ER). The excitation optical source was prepared by a high pressure mercury lamp (100 W, Olympus BH2-REL-T3) and a fluorescence mirror unit (Olympus U-MGFPHQ: excitation filter 460−480 HQ, absorption filter 495−540 HQ, Dichroic mirror 485).

IR Measurements. The nanotube hydrogel was lyophilized and subjected to IR measurement at 25 °C with a Fourier-transform IR spectrometer (Jasco FT-620) and an attenuated total reflection (ATR) accessory system (Diamond MIRacle, horizontal ATR accessory with a diamond crystal prism, PIKE Technologies, USA).

Spectroscopic Measurements. Fluorescence, UV/vis, and CD spectra of the fixed GFP and Mb in the nanotube hydrogel were measured at 25 °C using an F-4500 spectrophotometer (Hitachi) equipped with DCI temperature control (HAAKE), a U-3300 spectrophotometer (Hitachi) equipped with BU150A temperature control (YAMATO), and a J-820 spectropolarimeter (JASCO) equipped with PTC-423 L temperature control (JASCO), respectively.

Acknowledgment. This work was partly supported by Grant-in-Aid for Young Scientists (B) No. 21710117 from the Ministry of Education, Culture, Sports, Science and Technology (MEXT).

Supporting Information Available: Molecular packing analysis of the nanotubes by IR spectroscopy. Denaturation behavior of the fixed GFP in the nanotube hydrogel upon addition of urea. Influence of GdmCl on morphology of the nanotube encapsulating GFP in the hydrogel. Evaluation for the removal of the unencapsulated Mb from hydrogel D. Calibration curve of met-Mb. Monitoring for the auto oxidation of the fixed oxy-Mb into hydrogel D. This material is available free of charge via the Internet at http://pubs.acs.org.